COMPLEMENTARY EXPERIMENTAL AND SIMULATION-BASED CHARACTERIZATION OF TRANSIENT ARCS

M. Baeva[a], R. Methling[a], D. Gonzalez[a,*], D. Uhrlandt[a],
S. Gortschakow[a], A. Ehrhardt[b], S. Schmausser[b], O. Schneider[b]

[a] *Leibniz Institute for Plasma Science and Technology, Felix-Hausdorff-Strasse 2, 17489 Greifswald, Germany*

[b] *DEHN SE + Co KG, Hans-Dehn-Strasse 1, 92318 Neumarkt, Germany*

* diego.gonzalez@inp-greifswald.de

Abstract. Electric arcs generated by transient lightning-type surge currents in protection devices for low voltage appliances are studied by optical emission spectroscopy and spectra simulations. A surge pulse amplitude of 5 kA and 8/20 µs shape are applied. The arc radiation is recorded by a 3/4 m spectrometer and a high-speed camera equipped with metal interference filters for the O I (777 nm) and Hα (656 nm) lines. Absolute calibration was realized using a tungsten strip lamp. The arc images indicate a non-symmetrical shape. To determine the plasma properties, accompanying simulation solving the equation of radiative transfer for a given pressure and a temperature profile was carried out assuming local thermodynamic equilibrium. Line broadening due to the Stark effect is taken into account. The computed and measured spectra are compared. The conditions are varied until the measured and computed spectra match.

Keywords: Surge protection devices, spectroscopy, high-speed imaging, surge current pulses, over voltage, radiative transport.

1. Introduction

Surge protection devices (SPD) are widely used in electrical grids to suppress over voltages during transient conditions caused by voltage surges, therefore preventing damages of industrial or household devices. In low voltage power grids, SPDs can use the combination of different components including metal oxide varistors and spark gaps to limit transitory voltages up to levels of 1 kV (AC networks), to convert the surge pulse energy into heat, and to safely drain the resulting currents to the earthing system.

The working principle of spark gaps is to introduce a fault into the corresponding system leading to an arc with a burning voltage lower than the rated supply voltage. The ignited arc has to be nevertheless led to its extinction clearing the subsequent over-current and avoiding that it is further supplied by the power grid. To do that, the components of the spark gap shall permit to reach a considerable increment of the electric field of the arc by using different measures like arc elongation, wall cooling, arc splitting, magnetic blown-off or their combination.

The temporal development of the arc results from the interaction of electromagnetic, fluid, and heat transfer phenomena. The characterization of the plasma is often based on multiphysics models [1–4]. However, spectroscopic methods have been established already back in the past along with electrical measurements. The radiation emitted by the arc can be recorded in short times with a high spectral, spatial and temporal resolution. In cases where the results from spectroscopic measurements cannot directly provide knowledge of the plasma properties, complementary studies comprising modeling may be useful. The present work is aimed at characterizing the arc by means of measured and computed spectra. The experiments apply optical emission spectroscopy (OES). The spectra are computed by solving the equation of radiative transfer (ERT) along a line of sight using plasma temperature and pressure as adjustable parameters. The parameters are varied until measured and computed spectra reach an acceptable match.

2. Experimental setup and methods

A commercial SPD based on a spark gap (Fig. 1) was modified to enable the optical access. For that purpose, a side wall of the device under test (DUT) was replaced by a transparent window made of polycarbonate with good transmission properties for visible light. A framing camera (SIMD8-UV, Specialised Imaging) was used to record the temporal behaviour of the arc at different times. The SIM-camera can capture up to 8 frames with exposure times and adjustable interframe times down to a few ns.

A spatially resolved OES permits measurements by different time-windows of the current pulse. The optical emission spectroscopy was carried out using either a 1/2 m spectrometer or 3/4 m spectrometer for a higher resolution (SpectraPro 500i or 750, Roper Acton) that were equipped with ICCD cameras (PI Max 4, Princeton Instr.). Gratings with 150, 600 and 1200 l/mm were used. The measured spectra were absolutely calibrated by means of a tungsten-strip lamp. The apparatus profile of the 3/4 m spectrometer was
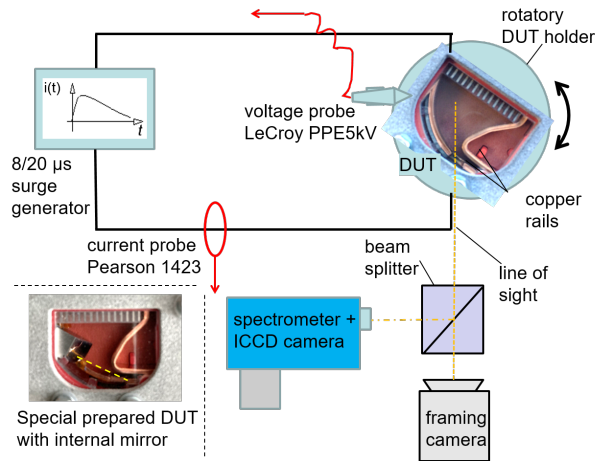
Figure 1. Experimental setup with its main components and a photograph of the DUT with the internal mirror.

obtained by means of a Tm hollow-cathode lamp. Owing the divergent characteristic of the copper running rails of the spark gap, a special DUT holder was constructed. It allows us to rotate the DUT and align the expected arc cross-section with respect to the line of sight. In addition, an in-house stainless-steel mirror was placed inside the arc chamber to determine the transversal intensity profile of the arc (see the lower side- left in Fig. 1). The surge current was supplied by a hybrid surge pulse generator, which delivers a standard 8/20 μs pulse according to IEC 62475.

3. Spectra computation

The spectral radiative intensity I_λ along a line of sight into direction s is described by the ERT, which in the case no scattering is written as [5]

$$\frac{dI_\lambda}{ds} = \kappa_\lambda B_\lambda - \kappa_\lambda I_\lambda, \tag{1}$$

where k_λ is the spectral absorption coefficient and B_λ is the Planck function. k_λ depends on the plasma composition, which is obtained assuming a local thermodynamic equilibrium (LTE). The spectral continuum is divided into emission from bound-free or radiative recombination and free-free or bremsstrahlung radiation resulting from the interaction of electrons with ions. The values of the Biberman-Norman and the Gaunt factors are taken equal to 1. Atomic and ionic spectral lines are taken into account. The NIST [6] database for spectral lines in the range (600–900) nm is used. For the calculation of the line profiles, other broadening mechanisms besides the Stark broadening are taken into account by means of a simplified model. It assumes that all lines have a Lorentzian profile. Its half-width splits into two parts. The first one acquires for all mechanisms except Stark broadening, e.g. Doppler and Van der Waals broadening. The second one represents the Stark broadening. Estimates show that the Stark broadening causes the dominant contribution.
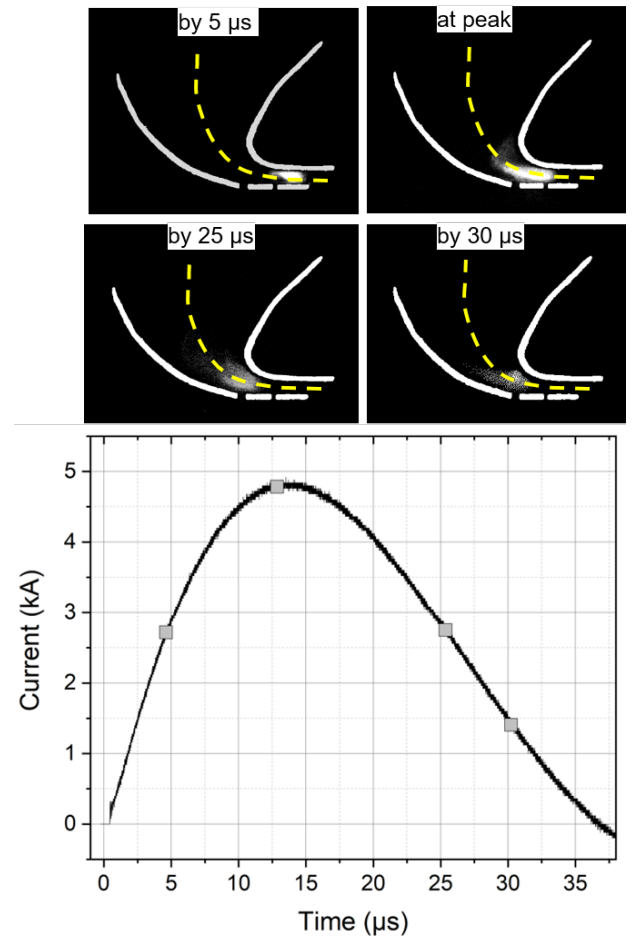
Figure 2. High-speed images (top) and arc current as function of time(bottom). The dash line indicates the path of the arc motion.

The ERT is solved in one dimension along a line of sight. The spectra computation starts with an initial guess of the profiles of the plasma temperature and pressure, and the corresponding equilibrium composition. The computed profiles include a convolution with the measured apparatus profile. Then, measured and computed spectra are compared and the plasma temperature and pressure are varied until agreement is achieved. Notice that due to the different impact of temperature and pressure on the spectra, the solution can considered as unambiguous.

4. Results and discussion

Figure 2 shows the course of arc current, and the corresponding images of the arc at different instants. In order to determine the spectral characteristics, the DUT was rotated aligning the arc cross-section and the slit of the spectrometer. Figure 3 shows the observed spectral distributions for different time windows according to those of Figure 2. Also the framing images in Figure 2 indicate that the arc shape is non-symmetric while it moves along the copper rails towards the splitter plates. The intensity distributions of the arc radiation in the visible range were first evaluated us-
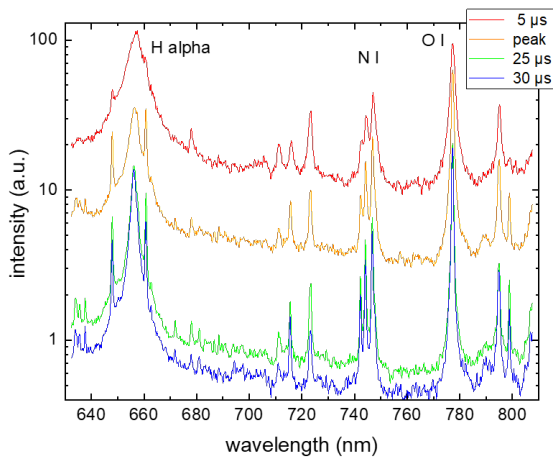
Figure 3. Recorded spectra from the arc at different instants along the dash line in Fig. 2

Figure 4. The 2-D spectrum to the instant of current peak (top, center) and side-on profile (bottom) along of the transversal arc section of the oxygen triplet at 777 nm.

ing the framing camera images (exposure times of 5 ns) at different intervals. Using the direction of the arc movement as tracking path, the intensity profiles were extracted from the images and fitted with double Gaussian profiles. The resulting curves indicate that the arc extends over a length that is larger than the depth of the spark gap (5 mm). Therefore, deviations from cylindrical symmetry must be expected in the arc cross section. This is confirmed by the observed two-dimensional spectrum of the O I-triplet at 777 nm obtained at the instant of the current peak, which is presented in Figure 4.

Mostly lines of N I and O I and in some experiments strong H_α lines were observed. Further lines that would for instance indicate the presence of copper released from the running-rails or carbon from the polymers in the chamber were not detected in a comparable intensity. As expected from the results with the framing camera, the side-on profile (Figure 4) indicates that the arc is compressed in the direction of movement. The front part of the arc shows a higher intensity and its section width is longer than the chamber depth (5 mm) confirming the deviation from a cylindrical symmetry. Thus there is not straightforward way for the determination of the emission coefficients for the exited levels by Abel-inversion and consequently, the plasma temperature and pressure cannot be determined. Furthermore, the observed exited levels of several nitrogen or oxygen species cannot be used for a meaningful determination of the plasma temperature from the Boltzmann plot technique also. A possible alternative was to combine the measured spectra with an iterative spectra computation of the O I-triplet at 777 nm since the triplet was well seen in all measurements.

The measured spectra were obtained in absolute intensities applying a calibration measurement with a tungsten strip lamp. Measurements with a hollow cathode emitter resulted in an apparatus profile of 0.03 nm for the used OES arrangement (3/4 m
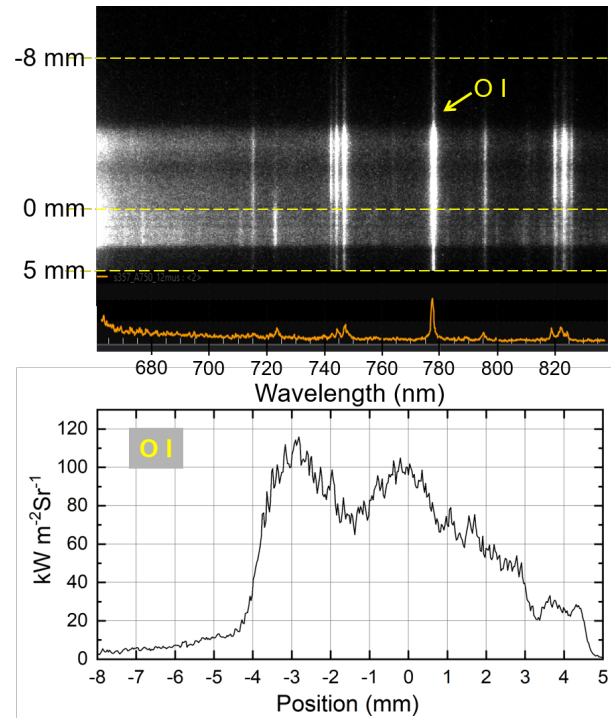
spectrometer). This ensured that the details of the O I-triplet were recorded with sufficient accuracy and that a overlapping of the individual components of the triplet was not the result of a too large apparatus profile. The spectral profile changes significantly depending on the instant of measurement and the current course. The intensity varies along the recording line while only slight changes in the profile are observed. Well pronounced maxima and minima similarly to that in the computed profiles are only found when the current decays below of the half-peak value i.e. after about 25 μs. Higher pressures and temperatures can therefore be assumed during the rise time of the current pulse, which lead to a relatively strong broadening of the line profile.

The simulation results have shown that the shape of temperature profile was of minor importance to the spectral intensity distribution. Instead, the maximum value of the plasma temperature and pressure played a role. Furthermore, an adjustment of the parameters for Stark broadening of the spectral lines was important. The best results were obtained with a value of $\Delta\lambda^S_{1/2} = 0.0028$ nm for the first and the third components of the triplet. $\Delta\lambda^S_{1/2} = 0.0025$ nm for the second component of the triplet. These values are taken at a temperature of 10000 K and electron density of 10^{22} m^{-3}. The line broadening parameters scale with the local values of temperature and electron density according to the relation given by Griem [7].

Experimental spectra recorded at several time win-
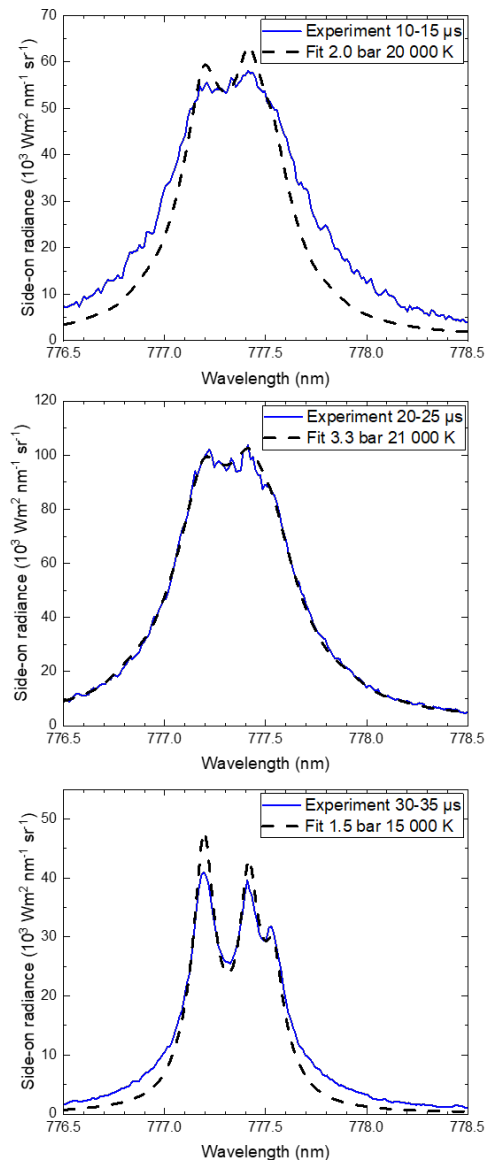
Figure 5. Comparison of measured (solid line) and computed spectral profiles (dashed line) of the O I-triplet at 777 nm at different time intervals during the pulse current (Figure 2): a) (10–15) µs, b) (20–25) µs, c) (30–35) µs.

dows were reproduced with sufficient accuracy. Since the plasma temperature affects mainly the spectral intensity while the plasma pressure affects mainly the width of the spectral line, the maximum temperature and pressure can be determined with accuracy of respectively ±1000 K and ±0.5 bar. The results of the spectra adjustments are shown in Figure 5. The measurement during the rise time of the current pulse was not evaluated since no consistent adjustment of the parameters along a suitable line of sight could be found. In this phase of the discharge, deviations from LTE could appear.

The discrepancy between measured and computed spectra to the time window (10–15) µs (Fig. 5a) i.e.

around current peak is probably caused by the fact that the integration times required for the measurement with high spatial and spectral resolution (5 µs) are quite long compared to the assumption of instantaneous parameters in the simulation. For that reason, rapid changes in the plasma parameters cannot be recorded with sufficient accuracy. Around the instant of current peak (Fig. 5a) and in particular during current decay (Fig. 5b) and (Fig. 5c), the assumption of LTE seems to be appropriate.

5. Conclusions

The physical properties of the plasma for a surge current arc of the form 8/20 µs (induced lightning stroke) with a peak value of 5 kA are studied in this work. Both the high-speed recordings and the side-on spectral distributions indicate an extended and non-symmetrical arc in the gas chamber.

Experimental studies employing optical emission spectroscopy and spectra simulation based on the solution of the equation of radiative transfer are carried out in order to characterize the arc. The arc plasma is assumed to be in the state of local thermodynamic equilibrium. The evaluation of the plasma temperature and pressure is based on the iterative adjustments of the computed and measured spectra for the triplet of O I at 777 nm.

The simulations are performed in a wide range of maximum temperatures (14000–23000) K and pressures up to 5 bar. The results obtained show that a good match can be found for the decaying current phase and a sufficient agreement around current peak. During the ignition phase and current rise, where a high pressure and deviations from equilibrium may appear, the combined approach is of limited accuracy.

References

[1] A. Gleizes, J. J. Gonzalez, and P. Freton. Thermal plasma modelling. *J. Phys. D.: Appl. Phys.*, 38(9):R153–R183, 2005. `doi:10.1088/0022-3727/38/9/R01`.

[2] P. Freton and J. J. Gonzalez. Overview of current research into low-voltage circuit breakers. *The Open Plasma Phys. J*, 2:105–119, 2009. `doi:10.2174/1876534300902010105`.

[3] F. Yang, Y. Wu, M. Rong, et al. Low-voltage circuit breaker arcs – simulation and measurements. *J. Phys. D.: Appl. Phys.*, 46(273001), 2013. `doi:10.1088/0022-3727/46/27/273001`.

[4] M. Lindmayer. Remarks concerning arc roots in CFD modellig of switching arcs. *Int. Conf. Electrical Contacts*, 2021.

[5] M. F. Modest. *Radiative heat transfer*. Elsevier Inc., Amsterdam, 2013. ISBN 978-0-12-386944-9.

[6] A. Kramida, Y. Ralchenko, J. Reader, and NIST ASD Team (2022). NIST Atomic Spectra Database (version 5.10), National Institute of Standards and Technology, Gaithersburg, MD., 2022.

[7] H. R. Griem. *Spectral line broadening by plasma*. Academic Press, New York and London, 1974. ISBN 9780323150941.